A Reduced Complexity Receiver for Multi-Carrier Faster-Than-Nyquist Signaling

Frank Schaich and Thorsten Wild
Bell Labs, Alcatel-Lucent, Germany.
Email: {frank.schaich, thorsten.wild}@alcatel-lucent.com

***Abstract*—Faster-than-Nyquist signaling originally proposed by J. E. Mazo promises higher spectral efficiencies by introducing controlled intersymbol interference at the transmitter at the cost of a higher receiver complexity. We propose a non-trellis based maximum likelihood (ML) receiver in conjunction with linear MMSE reception and interference cancellation for multi-carrier faster-than-Nyquist signaling (MC-FTN). The proposed receiver is able to collect the gains MC-FTN is promising while significantly reducing complexity compared to a receiver performing the optimum detection strategy (exhaustive search). We judge our receiver in terms of complexity, error rate performance and achieved spectral efficiency. The key question to be answered with respect to MC-FTN signaling in the view of a potential inclusion into a future 5G cellular communication system is: Are there scenarios in a realistic cellular communication setting for which gains from MC-FTN can be achieved at what complexity? This paper gives some insights covering all three aspects (scenarios, performance gains, complexity).**

***Index Terms*—Multicarrier Transmission, faster-than-Nyquist, FTN, maximum likelihood detection, interference cancellation, OFDM, MMSE**

I. Introduction

In 1975 J. E. Mazo laid the foundation for Faster-than-Nyquist (FTN) signaling [1]. He stated that it is possible to exceed Nyquist's border [2] while not increasing the bit error rate. Sounding disputable at first sight, the key aspect making this possible is the minimum Euclidean distance between all available signal sequences not shrinking for signaling rates (BPSK using sinc pulses) up to 25% higher than when obeying Nyquist's rule. So, with implementing a more complex reception scheme relying on sequence detection one is able to exploit this. Numerous groups have taken up on this topic: In [3] Rusek and Anderson introduced the two dimensional Mazo limit by extending the FTN principle to the frequency domain, paving the way for MC-FTN. In [4] the same group stated a doubling of the spectral efficiency of OFDM by applying MC-FTN in theory to be possible. A theoretical assessment of the achievable capacities can be found in [5]. A generalization with respect to the pulse design is presented in [6] and [7]. Additionally the former paper deals with constrained coding as a potential tool for improving FTN. Various publications dealing with signal reception e.g. based on sequence detection are available (e.g. [8]). A first connection between FTN and MIMO has been made in [13] and extended in [14].

Within this paper we propose a two-staged receiver structure not relying on trellis-detection. Instead, reception is symbol-by-symbol based, evaluating the squared Euclidean distance of the time domain signals. To reduce complexity a first stage applies linear reception followed by the determination of the reliability of the single subcarrier symbols and interference cancellation. This way the search space of the second stage may be significantly reduced.

The paper is structured as follows: chapter II presents the signal model followed by a detailed description of the detection principle in chapter III. In chapter IV we evaluate our system with respect to complexity, error rate performance and gains in spectral efficiency. We close the paper with an outlook and some general remarks on MC-FTN in the view of future cellular communication systems.

In the following, matrices and vectors use bold characters, the former capital the latter lowercase letters. $(.)^H$ and $(.)^{-1}$ are indicating hermitian and inverse operations.

II. Signal model

Fig. 1 depicts the cutout of a transmitted signal sequence when applying one-dimensional FTN signaling.

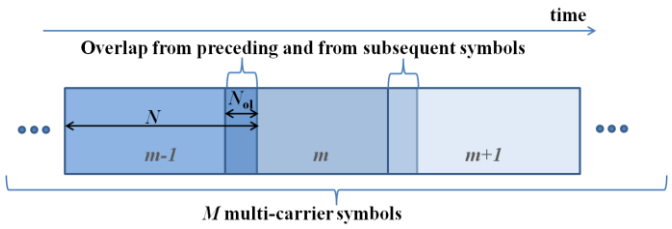

Fig. 1. Transmit signal sequence

The burst consists of M multi-carrier symbols overlapping in time (up to now we concentrate on one-dimensional FTN, i.e. no overlap in frequency direction). Consecutive bursts do not overlap. A single allocation may for example correspond to a single transmission time interval (TTI) as defined in LTE.

A single symbol consists of N samples, N_{ol} is the length of the overlap region. $m \in [1, M]$ accounts for all symbols within the burst of length M.

For simplicity we start with OFDM w/o cyclic prefix, i.e. a single rectangle in Fig. 1 corresponds to a single OFDM

symbol. Future work will extend this to systems applying filtered multi-carrier such as presented in [15] and [16].

Mathematically the time domain received signal for the AWGN channel for a single multicarrier symbol m of interest is as follows:

$$\boldsymbol{y}_m = \boldsymbol{F}_m \boldsymbol{s}_m + \boldsymbol{F'}_{m-1} \boldsymbol{s}_{m-1} + \boldsymbol{F'}_{m+1} \boldsymbol{s}_{m+s} + \boldsymbol{n} \quad (1)$$

$\boldsymbol{y}_m$ is the received symbol vector with complex entries and dimension Nx1 containing the useful signal (first term), interference from the preceding (second term), interference from the subsequent symbol (third term) and complex AWGN with zero mean and $\sigma^2/2$ per dimension. $\boldsymbol{s}_x$ (x: m-1, m, m+1) are the respective symbol vectors carrying complex QAM symbols ($\boldsymbol{s}_0$ and $\boldsymbol{s}_{M+1}$ are vectors containing only zeros). $\boldsymbol{F}_m$, $\boldsymbol{F'}_{m-1}$ and $\boldsymbol{F'}_{m+1}$ are the modulation matrices (e.g. for OFDM $\boldsymbol{F}_m$ equals the IDFT matrix $\boldsymbol{F}$ with dimension NxN, while $\boldsymbol{F'}_{m-1}$ and $\boldsymbol{F'}_{m+1}$ are composed as follows:

$$\boldsymbol{F'}_{m-1} = \begin{pmatrix} \boldsymbol{F}_C \\ \boldsymbol{0} \end{pmatrix} \quad \boldsymbol{F'}_{m+1} = \begin{pmatrix} \boldsymbol{0} \\ \boldsymbol{F}_A \end{pmatrix} \quad (2)$$

$\boldsymbol{0}$ is a (N-N_{ol})xN matrix containing zeros, $\boldsymbol{F}_A$ and $\boldsymbol{F}_C$ are N_{ol}xN submatrices of the IDFT matrix when structuring it as follows:

$$\boldsymbol{F} = \begin{pmatrix} \boldsymbol{F}_A \\ \boldsymbol{F}_B \\ \boldsymbol{F}_C \end{pmatrix} \quad (3)$$

III. Detection

Fig. 2 depicts the detector. Detection is performed symbol-by-symbol following the maximum likelihood (ML) principle. To keep complexity in check a linear pre-processing stage reduces the symbol space to be checked by the ML detector. A more detailed description follows. As part of the headings the range of m is given, for which the respective step is to be performed.

1) *Linear reception of the first symbol (m = 1)*

The detection process starts with transforming the first symbol (m = 1) to frequency domain using a comparatively simple linear filter:

$$\tilde{\boldsymbol{s}}_{m,x} = \boldsymbol{W}_x^{\boldsymbol{H}} \boldsymbol{y}_m \quad \text{with } x \in \{\text{MMSE}, \text{DFT}\}$$
$$\boldsymbol{W}_{MMSE} = \left(\boldsymbol{F}_m \boldsymbol{F}_m^{\boldsymbol{H}} + \boldsymbol{F'}_{m+1} \boldsymbol{F'}_{m+1}^{\boldsymbol{H}} + \sigma^2 \boldsymbol{I}\right)^{-1} \boldsymbol{F}_m \quad (4)$$
$$\boldsymbol{W}_{DFT} = \boldsymbol{F}_m^{-1}$$

$\boldsymbol{W}_{MMSE}$ follows the MMSE principle (Wiener filter), $\boldsymbol{W}_{DFT}$ simply applies the DFT matrix following the typical course of OFDM processing. Output to the next detection steps are the noisy symbol vectors $\tilde{\boldsymbol{s}}_{m,x}$ including inter-carrier interference. The latter originates from transforming the overlapping parts from the subsequent multi-carrier symbol to frequency domain.

2) *QAM symbol ranking for preselection (m = 1)*

The next step is to rank the single complex subcarrier symbols with respect to their reliability. Several variants to calculate reliability are possible:

- Squared Euclidean distance to the closest QAM symbol
- Distance to the closest decision threshold

Output of this step is a sorted list of noisy and interference afflicted complex QAM symbols.

Set m = 2 and go to step 3.

3) *QAM Symbol decision and interference cancellation ($m \in [2, M]$)*

The first symbol of the burst had no interference from preceding symbols. This does not hold for the following symbols. So, we either have to accept a higher grade of

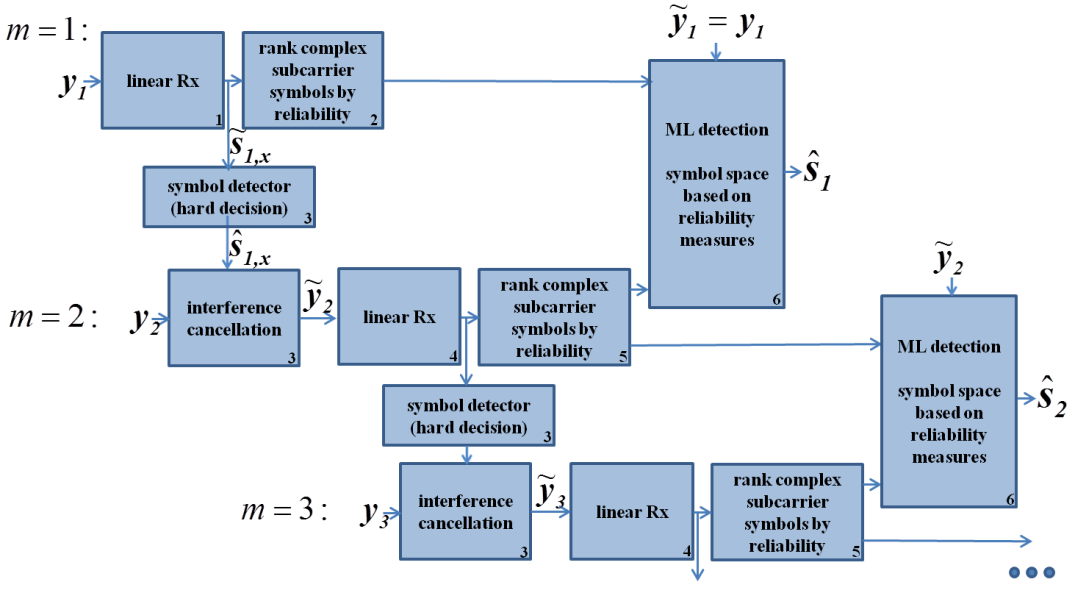

Fig. 2. ML based detector with linear preprocessing and interference cancellation for search space reduction

interference when performing linear reception or alternatively we make use of the results obtained so far and perform interference cancellation. To do so, we perform hard decision on $\tilde{\boldsymbol{s}}_{m-1,x}$ producing $\hat{\boldsymbol{s}}_{m-1,x}$, synthesize the time signal generated by these estimates and cancel the impact of the preceding symbol *m-1* to the actual one *m*:

$$\tilde{\boldsymbol{y}}_m = \boldsymbol{y}_m - \boldsymbol{F}'_{m-1}\hat{\boldsymbol{s}}_{m-1,x} \tag{5}$$

4) Linear reception of the mth symbol (m ∈ [2, M])

After having cancelled the interference from the preceding symbol, the next processing step is linear reception similar to step 1 for symbol *m*.

5) QAM symbol ranking for the mth symbol (m ∈ [2, M])

To further reduce the search space of the following ML detection, we rank the single subcarrier symbols of multi-carrier symbol *m* according to their reliability similar to step 2.

6) ML detection of the (m-1)th symbol (all m)

Input to the ML detector is the received signal vector (including interference from the next multi-carrier symbol) and the reliability ranking of the subcarrier symbols for the actual multi-carrier symbol and subsequent one. The ML detector is based on the squared Euclidean distance (a well-known substitute for the general ML rule in AWGN):

$$\hat{\boldsymbol{s}}_{m-1,ML} = \arg\min_{\boldsymbol{s}_{m-1},\boldsymbol{s}_m} \left|\tilde{\boldsymbol{y}}_{m-1} - \hat{\boldsymbol{y}}_{m-1}\right|^2 \tag{6}$$

$\tilde{\boldsymbol{y}}_{m-1}$ is the received signal without interference from the preceding one, but with interference from the subsequent on, $\hat{\boldsymbol{y}}_{m-1}$ the synthesized signal depending on the QAM symbol vectors $\boldsymbol{s}_{m-1}$ and $\boldsymbol{s}_m$. The lowest metric decides for the estimated symbol vector $\hat{\boldsymbol{s}}_{m-1,ML}$.

Then *m* is increased by 1 and the algorithm is continued with step 3 until all symbols are processed.

The number of metrics to be calculated in case of exhaustive search is as follows:

$$K_{\mathrm{ML,es}} = \left(K_{\mathrm{Mod}}\right)^{K_{\mathrm{scrr}}K_{\mathrm{MCSymb}}} \tag{7}$$

K_{Mod} is the number of available modulation symbols (e.g. QPSK: $K_{\mathrm{Mod}} = 4$), K_{scrr} the number of subcarriers carrying data and K_{MCSymb} the number of multi-carrier symbols contributing to the actually processed received symbol vector $\boldsymbol{y}_m$ ($K_{\mathrm{MCSymb}} = 2$ for the edge symbols, $K_{\mathrm{MCSymb}} = 3$ for the remaining ones). As someone would expect this number is too high for the detector to be implemented for typical values of K_{scrr} and K_{MCSymb}. However, as indicated above there are ways to significantly reduce the search space:

If the implemented multi-carrier system follows similar rules as e.g. LTE, K_{scrr} would be in the range of e.g. 600 and 1200, respectively. So, a way to make detection feasible is to convert the problem into several smaller sub-problems by applying a bank of filters, each cutting out a fraction of all subcarriers (e.g. $K'_{\mathrm{scrr}} = 24$). (E.g. the block-filtered multi-carrier signal format in [16] supports this.)

By making use of the ranking lists produced earlier we are able to even more reduce the problem. Instead of all subcarrier symbols we only vary the K''_{scrr} least reliable ones keeping the other fixed as given by $\hat{\boldsymbol{s}}_{m,x}$. To what extend we may drive this will be examined later.

K_{MCSymb} is typically equal to three, as interference from both the preceding and the subsequent multi-carrier symbol is present (exceptions are the first and the last symbol of the burst). However, by applying interference cancellation as outlined in step 3 we are able to achieve $K'_{\mathrm{MCSymb}} = 2$ in any case.

Finally we may reduce K_{Mod} due to the fact that the probability of a given received subcarrier symbol to be originated by a given modulation symbol is highly depending on its position within the complex plane (actual probabilities are given in a later section). The following figures depict this.

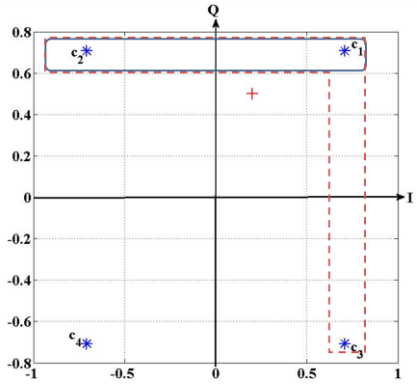

Fig. 3. Complex plane with received modulation symbol and considered candidate transmit symbols

The stars in Fig. 3 are the available modulation symbols, the plus exemplifies a single element of the received symbol vector $\tilde{\boldsymbol{s}}_{m,x}$ after linear processing (steps 1 and 4, respectively). According to its position it has been originated by [c_1, c_2, c_3, c_4] with declining probability. So, accepting wrong decisions to a minor extend we may reduce K_{Mod} to $K'_{Mod} = 3$ (dashed red box) or even 2 (continuous blue box) by only taking the respective closest modulation symbols into account when calculating the metrics. Especially with higher order modulations (16QAM, 64QAM) the complexity savings are tremendous by doing so.

A very attractive feature of the presented detection algorithm is its capability to be highly parallelized (metric calculations).

IV. RESULTS

We have conducted link level simulations to assess the performance of the presented scheme with respect to complexity reduction (compared to exhaustive search), error rate and spectral efficiency. As already stated the underlying signal format is OFDM. For now we consider the AWGN channel.

A. Complexity

We have assessed complexity in terms of number of metrics to be calculated following (5). We have chosen $K'_{\mathrm{scrr}} = 24$ assuming

- either a small band system with subcarrier spacings similar to LTE
- or a broadband system with comparatively wider subcarrier spacings
- or a cutout of a broadband system with subcarrier spacings similar to LTE with the help of filters as outlined earlier. For now we assume ideal filtering (i.e. subcarriers of interest are unchanged, the other subcarriers are perfectly suppressed).

As outlined earlier we are able to reduce the search space even more, by making use of the ranking lists produced in steps 2 and 5, respectively. Each sorted list includes erroneous and correct modulation symbols (if being decided at this stage) in a mixed order (with the erroneous ones accumulating at lower indices with reasonable system settings and channel conditions). To dimension K''_{scrr} we are interested in the statistical behavior of the indices of the erroneous symbols. Fig. 4 is depicting a respective exemplary CDF (cumulative distribution function).

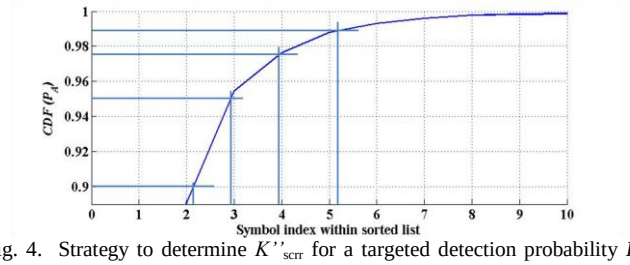

Fig. 4. Strategy to determine K''_{scrr} for a targeted detection probability P_A *(SNR =10dB, T_0/T = 1.085)*

P_A = [0.9, 0.95, 0.975, 0.99] means that we need to chose K''_{scrr} = [3, 3, 4, 6] to guarantee not to miss more than 1-P_A symbol errors in average (trusting on subsequent error correction and/or higher layer mechanisms like HARQ and ARQ to deal with the missed ones) by doing so.

Figs. 5a-d depict the exemplary K''_{scrr} depending on the grade of overlap quantified by T_0/T (SNR = 10 dB, QPSK, M = 6, N = 32, N_{ol} = [1, 2, 3, 4, 5]):

$$\frac{T_0}{T} = \frac{MN}{(M-1)(N-N_{ol})+N} \tag{8}$$

T is the time duration of the burst when applying FTN and T_0 the duration w/o overlap (and w/o cyclic prefix).

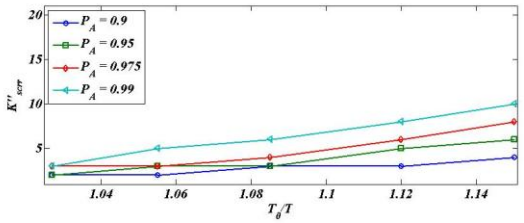

Fig. 5a. K''_{scrr} for MMSE based preselection using the distance to the closest decision threshold as reliability measure

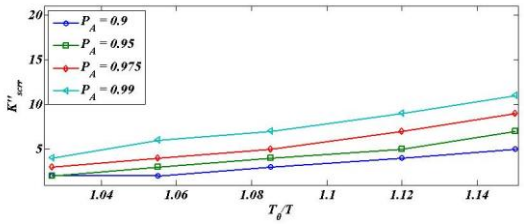

Fig. 5b. K''_{scrr} for MMSE based preselection using the distance to the closest constellation point as reliability measure

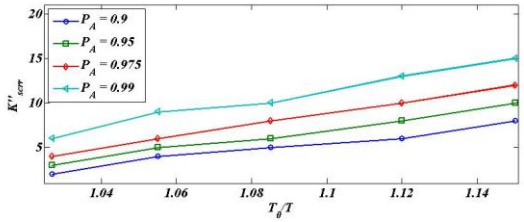

Fig. 5c. K''_{scrr} for DFT based preselection using the distance to the closest decision threshold as reliability measure

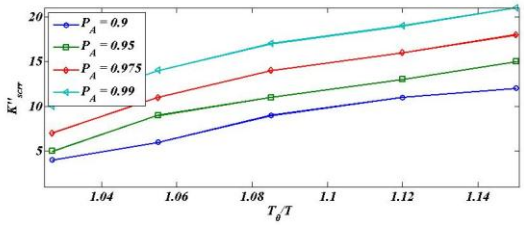

Fig. 5d. K''_{scrr} for DFT based preselection using the distance to the closest constellation point as reliability measure

Obviously, it is wise to spend a bit more complexity to generate the ranking lists (i.e. use MMSE based detection instead of DFT based) as then the complexity of the ML based step is by far lower (K''_{scrr} may be chosen much lower without performance loss). Additionally, using the distance to the closest decision threshold is more effective than the distance to the closest constellation point. Table I compares the complexity of the ML detection applying exhaustive search and the proposed algorithm with MMSE based preselection using the distance to the closest decision threshold as reliability measure (T_0/T = 1.085, P_A = 0.95, SNR = 10 dB, QPSK). The tremendous savings in complexity are obvious.

TABLE I
COMPARISON OF COMPLEXITY

Parameters	Number of metrics to be calculated
$K_{\mathrm{Mod}} = 4$, $K'_{\mathrm{scrr}} = 24$, $K_{\mathrm{MCSymb}} = 3$	2.23e43
$K'_{\mathrm{Mod}} = 4$, $K''_{\mathrm{scrr}} = 3$, $K'_{\mathrm{MCSymb}} = 2$	4096
$K'_{\mathrm{Mod}} = 3$, $K''_{\mathrm{scrr}} = 3$, $K'_{\mathrm{MCSymb}} = 2$	729
$K'_{\mathrm{Mod}} = 2$, $K''_{\mathrm{scrr}} = 3$, $K'_{\mathrm{MCSymb}} = 2$	64

With choosing $K'_{\mathrm{Mod}} < 4$ as depicted in Fig. 3 it

occasionally happens with probability 1-P_B that although it is part of the search space the ML detector may not be able to correct the respective symbol (e.g. with c_4 being transmitted and the diamond being received to stay with the example of Fig. 3). Table II gives exemplary probabilities P_B (again T_0/T = 1.085, SNR = 10 dB, QPSK, $K''_{\mathrm{scrr}} = 3$).

TABLE II
IMPACT OF K'_{MOD}

K'_{Mod}	P_B
4	1
3	0.9979
2	0.9913

So, increasing complexity by increasing K'_{Mod} is needless for the given setup.

B. QAM symbol error rate performance

Naturally, complexity is only one aspect to be considered. Of similar if not higher importance is the link performance in terms of modulation symbol errors depending on the SNR. Our decoding scheme has three potential sources of error:

- Erroneous QAM symbols not covered within the relevant part of the reliability list (1-P_A)
- Erroneous QAM symbols covered within the relevant part of the reliability list, but missed due to K'_{Mod}<4 (1-P_B)
- Residual errors after ML detection excluding errors resulting from the previous stages (P_{ML}), i.e. errors which would have occurred even with exhaustive search due to the noise

Thus, the overall symbol error rate (SER) is as follows ($P_{\mathrm{SER,MMSE}}$ is the symbol error rate after MMSE processing):

$$P_{SER} = P_{SER,MMSE} \cdot (1 - P_A) + P_{SER,MMSE} \cdot P_A (1 - P_B) + P_{ML} \tag{9}$$

To relate performance we have used the required SNR to achieve a given SER as measure. Fig. 6 depicts it with targets for the uncoded SER of 1% and 0.1%. These figures are providing insights about the required link budget compared to a system not applying FTN (QPSK, K'_{Mod} = 2, K'_{scrr} = 24, MMSE, distance to the closest decision threshold as reliability measure).

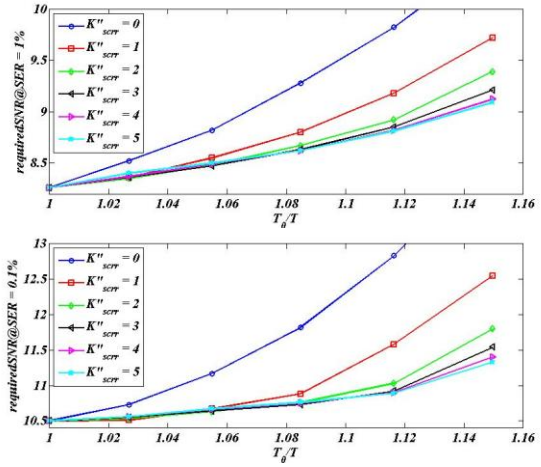

Fig. 6. Required SNR to achieve a given SER (1%, 0.1%) depending on the grade of overlap for various K''_{scrr}

The dark blue lines (circle) depict the performance, if only linear processing is applied (MMSE as described above). When additionally performing ML based detection, performance significantly improves. Obviously, with K''_{scrr} = 3 (black curve, triangle left) performance starts saturating in this case, i.e. by spending more complexity performance is improved only marginally. The error rate is dominated by the third term in (6) in this case.

C. Spectral efficiency

Finally, the performance measure we are interested in most is the gain in spectral efficiency we are achieving by applying FTN. The absolute spectral efficiency is calculated as follows:

$$S = S_0 r_l r_{\mathrm{FTN}} \tag{10}$$

S_0 is the inherent baseline spectral efficiency depending on the modulation order K_{Mod} and the code rate R_{FEC}.

$$S_0 = \frac{R_{\mathrm{FEC}} \log_2 K_{\mathrm{Mod}}}{T_S F_S} \tag{11}$$

T_S and F_S are symbol duration and subcarrier spacing, respectively ($T_S F_S = 0$). r_l is the normalized packet throughput in terms of received packets without error (i.e. treating erroneous packets as lost, relying on higher layer mechanisms alike HARQ and ARQ):

$$r_l = 1 - \mathrm{PER} \tag{12}$$

with the packet error rate PER depending on the symbol error rate (SER) and the number of modulation symbols per packet N_{Symbs}:

$$\mathrm{PER} = 1 - (1 - \mathrm{SER})^{N_{\mathrm{Symbs}}} \tag{13}$$

The remaining coefficient in (10) is taking into account the application of FTN ($r_{\mathrm{FTN}} = T_0/T$ as defined in (8)).

For the figure we have related the absolute spectral efficiencies S to the respective spectral efficiency S_{OFDM} of an equivalent system not applying FTN and w/o cyclic prefix (as we are interested in the gains through FTN, not through the avoidance of the cyclic prefix).

Fig. 7 depicts these ratios for K''_{scrr} = 3, K'_{Mod} = 2 and N_{Symbs} = 72 otherwise the same system settings as in the former section are holding.

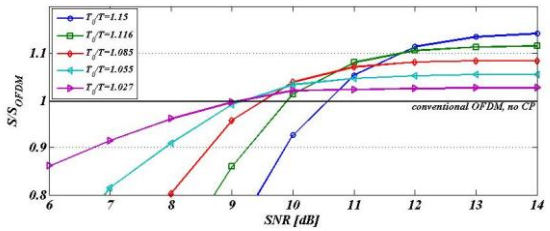

Fig. 7. Relative spectral efficiency of the proposed system applying FTN

As expected, once a given SNR is exceeded the system applying FTN exceeds the conventional system. The higher the overlap ratio T_0/T the later the turning point arrives, but the higher the ultimate throughput gain gets.

V. OUTLOOK AND GENERAL REMARKS

This paper introduces a novel approach to deal with MC-FTN (one-dimensional). We have presented a detection

algorithm relying on ML detection with reduced complexity through smart preprocessing. We have shown, that the detector is able to collect the gains MC-FTN is promising with significant savings in complexity.

There is a plethora of aspects open for future research. Just to name the most important ones:

- Extension to higher order modulations (16QAM, 64QAM) and introduction of forward error correction (FEC) with iterative knowledge exchange between the detector and the outer FEC decoder.
- Comparison with a system being highly adaptive with respect to the modulation scheme and code rate (MCS), as the ultimate performance metric of relevance is the distance of the envelope of the respective spectral efficiencies to the Shannon limit of a system w/ and w/o FTN.
- Filtered multi-carrier instead of OFDM and the impact of the underlying waveform in improving the linear preselection stage.
- Non-ideal filtering for breaking up the problem into several smaller ones.
- The application of constrained coding and its impact in improving the ML detection.
- Inclusion of more realistic channel models to determine the limits of applying FTN (mobility and delay spread)
- The extension of the simulation framework from the link level to a full-blown cellular system setting.
- The extension of the scheme targeting the two-dimensional Mazo limit.
- Information theoretic treatment of the proposed principles.
- PAPR (MC-FTN is worse than conventional OFDM) and means to improve it.
- Multi-antenna processing

Finally, before we close, some general remarks about MC-FTN as presented here with the following question in mind: Are there scenarios in a realistic cellular communication setting for which MC-FTN may be applied successfully?

Even with the reduction of complexity as presented here, receive processing still is rather complex. So, MC-FTN might not be a candidate for being the basic waveform of a novel cellular communication system (5G). However, counting on Moore's law MC-FTN may be a special mode for UL (here, complexity resides at the base station) and for DL serving high-end smartphones and pads by the time 5G is to be implemented.

The application of MC-FTN, if designed aggressively, drives the system towards its ISI limit. So, MC-FTN requires rather stable channel conditions (static up to nomadic) with very low delay spread. Therefore, MC-FTN may be applied mainly for static cell-center UEs (e.g. users streaming videos in mall/park close to serving point).

ACKNOWLEDGMENT

Part of this work has been performed in the framework of the FP7 project ICT-317669 METIS, which is partly funded by the European Union. The authors would like to acknowledge the contributions of their colleagues in METIS, although the views expressed are those of the authors and do not necessarily represent the project.

REFERENCES

[1] J. E. Mazo, "Faster-than-Nyquist Signaling," Bell Syst. Tech. Journal, vol. 54, pp. 1451-1462, Oct. 1975

[2] J. G. Proakis, "Chapter Nine: Signal Design for Band-Limited Channels," in *Digital Communications, 4*th ed. McGraw-Hill, Singapore 2001

[3] Rusek, F.; Anderson, J.B.; , "The two dimensional Mazo limit," *Information Theory, 2005. ISIT 2005. Proceedings. International Symposium on* , vol., no., pp.970-974, 4-9 Sept. 2005

[4] Anderson, John B.; Rusek, Fredrik; , "Improving OFDM: Multistream Faster-than-Nyquist Signaling," *Turbo Codes&Related Topics; 6th International ITG-Conference on Source and Channel Coding (TURBOCODING), 2006 4th International Symposium on* , vol., no., pp.1-5, 3-7 April 2006

[5] Rusek, F.; Anderson, J.B.; , "Constrained Capacities for Faster-Than-Nyquist Signaling," *Information Theory, IEEE Transactions on* , vol.55, no.2, pp.764-775, Feb. 2009

[6] Liveris, A.D.; Georghiades, C.N.; , "Exploiting faster-than-Nyquist signaling," *Communications, IEEE Transactions on* , vol.51, no.9, pp. 1502- 1511, Sept. 2003

[7] Jing Zhou; Daoben Li; Xuesong Wang; , "Generalized faster-than-Nyquist signaling," *Information Theory Proceedings (ISIT), 2012 IEEE International Symposium on* , vol., no., pp.1478-1482, 1-6 July 2012

[8] Prlja, A.; Anderson, J.B.; Rusek, F.; , "Receivers for Faster-than-Nyquist signaling with and without turbo equalization," *Information Theory, 2008. ISIT 2008. IEEE International Symposium on* , vol., no., pp.464-468, 6-11 July 2008

[9] Dasalukunte, D.; Rusek, F.; Owall, V.; , "An Iterative Decoder for Multicarrier Faster-Than-Nyquist Signaling Systems," *Communications (ICC), 2010 IEEE International Conference on* , vol., no., pp.1-5, 23-27 May 2010

[10] Dasalukunte, D.; Rusek, F.; Owall, V.; , "Multicarrier Faster-Than-Nyquist Transceivers: Hardware Architecture and Performance Analysis," *Circuits and Systems I: Regular Papers, IEEE Transactions on* , vol.58, no.4, pp.827-838, April 2011

[11] Kim, Y.J.D.; Bajcsy, J.; , "Iterative receiver for faster-than-Nyquist broadcasting," *Electronics Letters* , vol.48, no.24, pp.1561 -1562, November 22 2012

[12] McGuire, M.; Sima, M.; , "Discrete Time Faster-Than-Nyquist Signalling," *Global Telecommunications Conference (GLOBECOM 2010), 2010 IEEE* , vol., no., pp.1-5, 6-10 Dec. 2010

[13] Rusek, F.; , "A First Encounter with Faster-than-Nyquist Signaling on the MIMO Channel," *Wireless Communications and Networking Conference, 2007.WCNC 2007. IEEE* , vol., no., pp.1093-1097, 11-15 March 2007

[14] Rusek, F.; , "On the existence of the Mazo-limit on MIMO channels," *Wireless Communications, IEEE Transactions on* , vol.8, no.3, pp.1118-1121, March 2009

[15] Farhang-Boroujeny, B.; , "OFDM Versus Filter Bank Multicarrier," *Signal Processing Magazine, IEEE* , vol.28, no.3, pp.92-112, May 2011

[16] V. Vakilian, T. Wild, F. Schaich, S. ten Brink, Jean-Francois Frigon, "Universal-Filtered Multi-carrier Technique for Wireless Systems beyond LTE", submitted to IEEE PIMRC'13, London, September 2013